Emx2 directs the development of diencephalon in cooperation with *Otx2*

Yoko Suda[1,2,3,*], Zakir M. Hossain[1,*], Chiyoko Kobayashi[1], Osamu Hatano[4], Michio Yoshida[1], Isao Matsuo[1] and Shinichi Aizawa[1,3,*]

[1]Department of Morphogenesis, Institute of Molecular Embryology and Genetics (IMEG), Kumamoto University, Japan
[2]CREST, JST, Japan
[3]Vertebrate Body Plan Group, RIKEN Center for Developmental Biology, 2-2-1 Honjo, Kumamoto-860-0811, Japan
[4]Department of Anatomy, Nara Medical University, 840 Saijo-machi, Kashihara, Nara-634-8521, Japan
*These authors contributed equally to this work.

‡Author for correspondence (e-mail: saizawa@gpo.kumamoto-u.ac.jp)

SUMMARY

The vertebrate brain is among the most complex biological structures of which the organization remains unclear. Increasing numbers of studies have accumulated on the molecular basis of midbrain/hindbrain development, yet relatively little is known about forebrain organization. Nested expression among *Otx* and *Emx* genes has implicated their roles in rostral brain regionalization, but single mutant phenotypes of these genes have not provided sufficient information. In order to genetically determine the interaction between *Emx* and *Otx* genes in forebrain development, we have examined *Emx2*^{−/−}*Otx2*^{+/−} double mutants and *Emx2* knock-in mutants into the *Otx2* locus (*Otx2*[+/Emx2]). *Emx2*^{−/−}*Otx2*^{+/−} double mutants did not develop diencephalic structures such as ventral thalamus, dorsal thalamus/epithalamus and anterior pretectum. The defects were attributed to the loss of the *Emx2*-positive region at the three- to four-somite stage, when its expression occurs in the laterocaudal forebrain primordia. Ventral structures such as the hypothalamus, mammillary region and tegmentum developed normally. Moreover, dorsally the posterior pretectum and posterior commissure were also present in the double mutants. In contrast, *Otx2*[+/Emx2] knock-in mutants displayed the majority of these diencephalic structures; however, the posterior pretectum and posterior commissure were specifically absent. Consequently, development of the dorsal and ventral thalamus and anterior pretectum requires cooperation between *Emx2* and *Otx2*, whereas *Emx2* expression is incompatible with development of the commissural region of the pretectum.

Key words: Emx, Otx, Diencephalon, Forebrain development, Mouse

INTRODUCTION

Initial regionalization of the neural plate along its anterior-posterior axis occurs concurrent with, or shortly after, neural induction. Recent studies have suggested that anterior neuroectoderm is induced by permissive and instructive signals from anterior visceral endoderm, anterior definitive mesendoderm and others (Ang et al., 1996; Thomas and Beddington, 1996; Beddington and Robertson, 1998; Beddington and Robertson, 1999; Shawlot et al., 1999; Tam and Steiner, 1999; Kimura et al., 2000). *Otx2*, *Rpx/Hesx1* and *Six3* are the genes expressed in the early anterior neuroectoderm after induction (Suda et al., 1999; Martinez-Barbera et al., 2000a; Martinez-Barbera et al., 2000b; Wallis and Muenke, 2000). The initial morphological landmark of regionalization in the anterior neuroectoderm is the preotic sulcus, which corresponds to the future boundary between rhombomeres r2 and r3. This landmark becomes apparent around the three-somite stage. No molecular devices are known in the establishment of the boundary or initial development of r1 and r2. Rostral to the preotic sulcus, the midbrain/hindbrain junction (or isthmus) establishes molecularly around the six-

somite stage (Crossley and Martin, 1995; Millet et al., 1999; Suda et al., 1999) and morphologically around 9.0 days post coitus (dpc). A growing number of molecular studies have been conducted on developmental patterning of the midbrain and the establishment of the isthmus. *Otx2* and *Otx1*, *Pax2* and *Pax5*, and *En1* and *En2* cooperate in midbrain development (Hanks et al., 1995; Acampora et al., 1997; Acampora et al., 1998; Acampora et al., 1999; Suda et al., 1996; Suda et al., 1997; Suda et al., 1999; Urbanek et al., 1997; Schwarz et al., 1999). *Wnt1* functions to maintain the midbrain, possibly via the regulation of *En* expression (McMahon et al., 1992; Danielian and McMahon, 1996). The isthmus is established where *Otx2* and *Gbx2* meet (Wassarman et al., 1997; Broccoli et al., 1999; Hidalgo-Sanchez et al., 1999; Millet et al., 1999; Simeone, 2000), and plays an essential role in the rostrocaudal patterning of the midbrain. A loop of mutual interactions between *Fgf8*, *En1*, *En2*, *Pax2*, *Pax5* and *Wnt1* genes has been suggested in the isthmus (Balley-Cuif and Wassef, 1995; Joyner, 1996). Fibroblast growth factor (FGF8) is currently the sole factor demonstrating midbrain patterning activity of the isthmus (Crossley et al., 1996; Lee et al., 1997; Martinez et al., 1999).

In contrast, the mechanisms that delineate the telencephalon

and diencephalon are poorly understood. The forebrain or primary procencephalon segregates into the diencephalon and secondary procencephalon, from which alar plates protrude to generate the telencephalon. The boundary between the mesencephalon and diencephalon has been proposed to occur around the ten-somite stage, at the point where *Pax6* expression segregates from that of *Pax2* and *En1* (Araki and Nakamura, 1999; Schwarz et al., 1999; Matsunaga et al., 2000). The posterior commissure, which is formed near 10.5 dpc, is the morphological landmark of its dorsal boundary. Zona limitans interthalamica (zlth), which divides the ventral and dorsal thalamus, is formed earlier. It occurs molecularly near the five-somite stage and morphologically at 10.0 dpc, approximately where axial mesoderm is subdivided into the prechordal plate and notochord (Figdor and Stern, 1993; Shimamura et al., 1995; Inoue et al., 2000). The diencephalic region caudal to zlth is compatible with transformation into a mesencephalic phenotype by ectopic transplantation of isthmus/FGF8-soaked beads and by ectopic *En* expression (Crossley et al., 1996; Araki and Nakamura, 1999; Martinez et al., 1999). Sonic hedgehog (SHH) is expressed by zlth (Erickson et al., 1995), and it has been suggested that zlth functions not only as a barrier to restrict cell mixing and the spread of pattern information, but also as a source of morphogenetic information or as a local organizing center (Balley-Cuif and Wassef, 1995).

A number of genes are now known to be expressed in specific domains of the forebrain, and a neuromeric organization of the forebrain has been proposed (Bulfone et al., 1993; Shimamura et al., 1995; Shimamura et al., 1997). *Otx2*, *Otx1*, *Emx2* and *Emx1*, mouse cognates of *Drosophila* head gap genes, *otd* and *ems*, are among these genes. *Otx2* expression occurs throughout the anterior neuroectoderm during the initial phase of its induction. At 10.5-12.5 dpc, *Otx2* expression regresses in the dorsal telencephalon corresponding to the presumptive cerebral cortex (Simeone et al., 1993; Mallmaci et al., 1996). *Otx1* expression is evident around the 1 somite stage. At 10.25-12.5 dpc, *Otx1* expression covers the region from the cerebral cortex to the midbrain (Simeone et al., 1993). *Emx2* expression is evident around the three-somite stage. At 10.5-12.5 dpc, *Emx2* expression ranges from a portion of the subcortical domain in the telencephalon to the diencephalon rostral to zlth (Simeone et al., 1992a; Shimamura et al., 1997; Mallamaci et al., 1998). *Emx1* expression occurs in the cortical region around 9.5 dpc. As a result, *Otx2*, *Otx1*, *Emx2* and *Emx1* genes constitute a 'nested' expression, and the roles of these genes in brain regionalization have been suggested (Simeone et al., 1992b).

However, the phenotype of each single mutant of these genes has not been informative with respect to their roles in rostral brain regionalization. *Otx2*$^{-/-}$ mutants fail to develop a rostral head by the loss of earlier *Otx2* functions in visceral endoderm (Acampora et al., 1995; Matsuo et al., 1995; Ang et al., 1996; Rhinn et al., 1998; Kimura et al., 2000). Defects are apparent exclusively in the archipallium in *Emx2*$^{-/-}$ mutants (Pellegrini et al., 1996; Yoshida et al., 1997). *Otx1*$^{-/-}$ and *Emx1*$^{-/-}$ single mutants exhibit only subtle defects (Suda et al., 1996; Acampora et al., 1996; Qiu et al., 1996; Yoshida et al., 1997). In contrast, data from *Otx1* and *Otx2* double heterozygous mutants (*Otx1*$^{+/-}$*Otx2*$^{+/-}$) indicate that *Otx2* and *Otx1* cooperate in developing mesencephalon and posterior diencephalon at the time of brain regionalization (Acampora et al., 1997; Suda et al., 1997).

In the present study, we have generated *Emx2* homozygous and *Otx2* heterozygous double mutants (*Emx2*$^{-/-}$*Otx2*$^{+/-}$), and *Emx2* knock-in mutants into the *Otx2* locus (*Otx2*$^{+/Emx2}$), in order to genetically determine the interaction between *Emx2* and *Otx2* genes in forebrain development. *Otx2*$^{-/-}$ homozygous mutants exhibit defects caused by the lack of early *Otx2* function, as described above. Consequently, interactions between the two genes in brain regionalization could not be evaluated in the *Emx2*$^{-/-}$*Otx2*$^{-/-}$ double homozygous mutant state. Nevertheless, *Emx2*$^{-/-}$*Otx2*$^{+/-}$ double mutants demonstrate that these two genes indeed play crucial roles in the development of the ventral and dorsal thalamus, and anterior pretectum (precommissural region of pretectum; Martinez and Puelles, 2000). *Emx2* ectopic expression by its knock-in into the *Otx2* locus results in a phenotype complementary to the double mutants; *Emx2* expression must be suppressed for the development of the posterior pretectum (commissural region of the pretectum).

MATERIALS AND METHODS

Construction of knock-in vector

Emx2 (762 bp) cDNA lacking 3′UTR was isolated from a 11.5 dpc mouse cDNA library. The neomycin resistance gene (*neo*^{r}), which has no polyadenylation signal and is driven by the *Pgk1* promoter, was flanked by *loxP* sequences (see Fig. 6A). These sequences (*Emx2-loxp/neo/loxp*) were inserted into the *Nla*III site at the initial codon of the *Otx2* gene. The in-frame ligation was confirmed by nucleotide sequencing. Lengths of the homologous regions were 6.9 kb and 4.1 kb at the 5′ and 3′ sides of the insert (*Emx2-loxp/neo/loxp*), respectively, in the targeting vector. The diphtheria toxin-A fragment (*DT-A*) gene, driven by the MC1 promoter, was used for negative selection of homologous recombinants as described (Yagi et al., 1993b). (The details of vector construction can be provided upon request.)

Generation of mutant mice

TT2 ES cells (Yagi et al., 1993a) were cultured, electroporated with *Sal*I linearized targeting vector and selected against G418 as described (Nada et al., 1993; Yagi et al., 1993b). Homologous recombinants were assessed by long-PCR with a sense primer, p1 (5′-ATCGCCTTCTTGACGAGTTCTTCTG), in the *neo*^{r} gene and an antisense primer, p2 (5′-CTTATAATCCAAGCAATCAGTGG-TTGAG), in the *Otx2* genome located downstream of the 3′ end of the homologous region in the targeting vector (see Fig. 6A). Homologous recombinants were obtained at a frequency of 115 of 120 G418 resistant clones. Recombinants were confirmed by Southern blot hybridization using probes in the *neo*^{r} gene and in the third exon of the *Otx2* genome (*Sph*I/*Hin*dIII fragment in Fig. 6A). Chimeric mice were obtained through injection of targeted TT2 cells into eight-cell stage embryos, as described (Yagi et al., 1993b). Chimeras were crossed with *Cre* females, which expressed Cre in their zygotes (Sakai and Miyazaki, 1997), in order to generate F$_1$ heterozygotes. *Otx2* and *Emx2* heterozygotes were obtained as described (Matsuo et al., 1995; Suda et al., 1996; Yoshida et al., 1997). The genetic background of animals used in the present study is noted in Results. Mice were housed in environmentally controlled rooms of the Laboratory Animal Research Center of Kumamoto University under University guidelines for animal and recombinant DNA experiments.

Genotyping of mice

Genotypes of newborn mice and embryos were routinely determined by PCR analyses. Confirmation, when necessary, was by Southern

blot analyses. Genomic DNAs used in the analyses were prepared from tails or yolk sacs. In PCR analysis, knock-in alleles, which retained or lost the *neo*[r] gene, were detected as the 2.1 and 0.7 kb PCR products, respectively. A sense primer, p3 (5′-CCGAGAGTTTCCTT-TTGCACAACGC), was placed in the *Emx2* cDNA and an antisense primer, p4 (5′-TGTGGCACTCGGCAGTTTGGTAGC), was in the first exon of the *Otx2* genome (see Fig. 6A). Genotypes of *Otx2* and *Emx2* knockout alleles were identified as described previously (Matsuo et al., 1995; Suda et al., 1996; Yoshida et al., 1997).
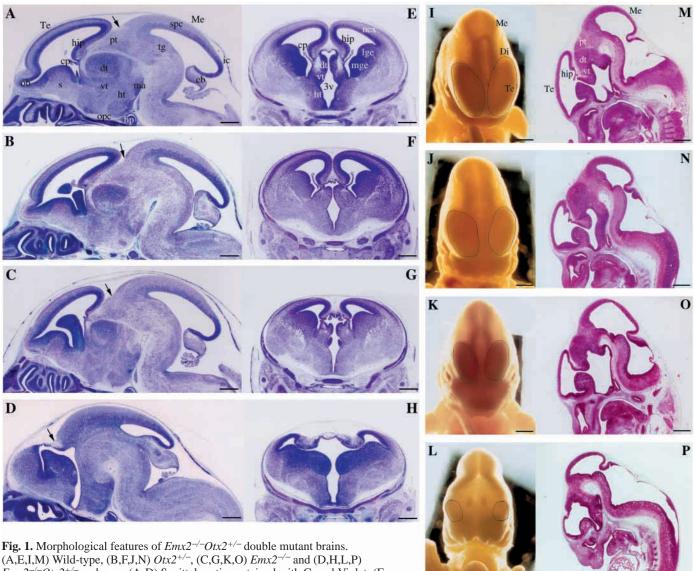
Histological analysis

Mouse embryos were fixed with Bouin's fixative solution at room temperature for 18-24 hours. Specimens were subsequently dehydrated and embedded in paraplast. Serial sections (8 μm) were prepared and stained with Hematoxylin and Eosin or with 0.1% Cresyl Violet (Sigma).
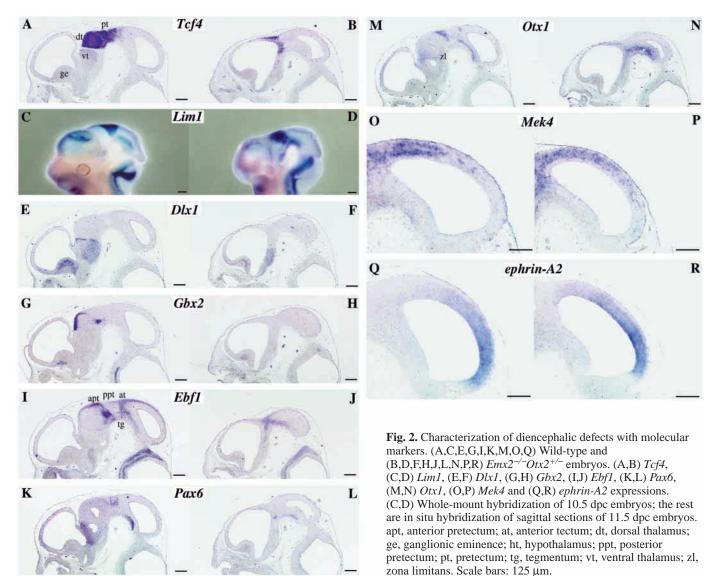
RNA probes and in situ hybridization

Embryos were dissected in PBS and fixed overnight at 4°C in 4% paraformaldehyde (PFA) in PBS. Specimens were gradually dehydrated in methanol/PBT (PBS containing 0.1% Tween-20) up to 100% methanol and stored at −20°C. The protocol for in situ hybridization of embryos was as described previously (Wilkinson, 1993). Single-stranded digoxigenin-UTP-labeled (Boehringer Mannheim) RNA probes were used. The probes were as described for *Wnt1* and *Wnt7b* (McMahon and Bradley, 1990), *BF1* (*Foxg1* – Mouse Genome Informatics; Tao and Lai, 1992), *En1* and *En2* (Davis and Joyner, 1988), *Pax2* (Dressler et al., 1990), *Pax5* (Asano and Gruss, 1992), *Pax6* (Walther and Gruss, 1991), *Dlx1* (Bulfone et al., 1993), *Fgf8* (Crossley and Martin, 1995), *Otx1* and *Otx2* (Matsuo et al., 1995), *Gbx2* (Bulfone et al., 1993), *Six3* (Oliver et al., 1995), *Tcf4* (Korinek et al.,1998), *ephrin-A2* (Efna1 – Mouse Genome Informatics; Flenniken et al., 1996), *Mek4* (Cheng and Flanagan,

Fig. 1. Morphological features of *Emx2*^{−/−}*Otx2*^{+/−} double mutant brains. (A,E,I,M) Wild-type, (B,F,J,N) *Otx2*^{+/−}, (C,G,K,O) *Emx2*^{−/−} and (D,H,L,P) *Emx2*^{−/−}*Otx2*^{+/−} embryos. (A-D) Sagittal sections stained with Cresyl Violet, (E-H) frontal sections stained with Cresyl Violet and (M-P) sagittal sections stained with Hematoxylin and Eosin. (I-L) Dorsal views of embryos. (A-H) 15.5 dpc, (I-P) 12.5 dpc. Arrows in A-D indicate the position of posterior commissure; circles in I-L indicate cerebral hemispheres. cb, cerebellum; cp, choroid plexus; Di, diencephalon; dt, dorsal thalamus; ept, epithalamus; hip, hippocampus; hp, hypophysis; ht, hypothalamus; ic, inferior coliculus; lge, lateral ganglionic eminence; ma, mammillary region; Me, mesencephalon; met, metencephalon; mge, medial ganglionic eminence; ncx, neocortex; ob, olfactory bulb; opc, optic chiasma; pt, pretectum; s, septum; spc, superior coliculus; Te, telencephalon; tg, tegmentum; vt, ventral thalamus; 3v, the third ventricle. Scale bars: 500 μm.

Fig. 2. Characterization of diencephalic defects with molecular markers. (A,C,E,G,I,K,M,O,Q) Wild-type and (B,D,F,H,J,L,N,P,R) $Emx2^{-/-}Otx2^{+/-}$ embryos. (A,B) *Tcf4*, (C,D) *Lim1*, (E,F) *Dlx1*, (G,H) *Gbx2*, (I,J) *Ebf1*, (K,L) *Pax6*, (M,N) *Otx1*, (O,P) *Mek4* and (Q,R) *ephrin-A2* expressions. (C,D) Whole-mount hybridization of 10.5 dpc embryos; the rest are in situ hybridization of sagittal sections of 11.5 dpc embryos. apt, anterior pretectum; at, anterior tectum; dt, dorsal thalamus; ge, ganglionic eminence; ht, hypothalamus; ppt, posterior pretectum; pt, pretectum; tg, tegmentum; vt, ventral thalamus; zl, zona limitans. Scale bars: 125 µm.

1994), *Lim1* (Lhx – Mouse Genome Informatics; Fujii et al., 1994), *Ebf1* and *Ebf3* (Garel et al., 1997), and *COUP-TFI* (Nr2f1 – Mouse Genome Informatics; Qiu et al., 1994). A 3′UTR probe was used as described (Yoshida et al., 1997) in order to detect endogenous *Emx2* expression in knock-in mutants. A cDNA probe was used for the detection of both endogenous and ectopic *Emx2* expression.

Immunohistochemistry

The peptide of 50 amino acid residues (EMX2-C50) from the C-terminal of mouse EMX2 protein was chemically synthesized. The rabbit anti-EMX2-C50 antiserum was obtained with the peptide as described (Tanaka et al., 1991). The antiserum was absorbed with mouse liver powder and used at the dilution of 1:2000 in PBS containing 1% goat serum. Paraffin sections of embryos were prepared as described (Gurdon et al., 1976; Mallamaci et al., 1996). Sections were deparafinized in xylene. Subsequently, specimens were rehydrated and incubated with 4% blocking serum for 1 hour, followed by incubation with antibodies. EMX2 expression was detected with rabbit anti-mouse EMX2-C50 antiserum and the secondary antibody (biotinylated goat anti-rabbit IgG) at 1:200 dilution. Posterior commissure neurons were detected with anti-mouse GAP43 monoclonal antibody (Sigma) at a dilution of 1:2000 and horseradish peroxidase-labeled secondary antibody (goat anti-

mouse IgG, ZYMED, USA) at a dilution of 1:500. Chromogenic staining was effected according to the protocol supplied by the manufacturer (VECTASTAIN Elite ABC kit, Vector Laboratories).

RESULTS

Morphological features of double mutant brain

Genetic background influences the phenotype of *Otx2* heterozygous mutants (Matsuo et al., 1995). Our ES cells, TT2, were derived from an F_1 embryo between C57BL/6 and CBA mice. *Otx2* is expressed in cephalic neural crest cells (Kimura et al., 1997), and F_1 *Otx2* heterozygotes obtained from crosses of chimeras with C57BL/6 females exhibit craniofacial defects, yielding few fertile heterozygotes. F_1 heterozygotes that resulted from mating chimeras with CBA females did not possess the defects. Consequently, *Otx2* heterozygotes have been maintained by crosses with CBA mice. Accordingly, *Emx2* heterozygotes employed in this study were obtained via crosses of chimeras with CBA females and have been maintained by crosses with CBA mice (Yoshida et al., 1997;
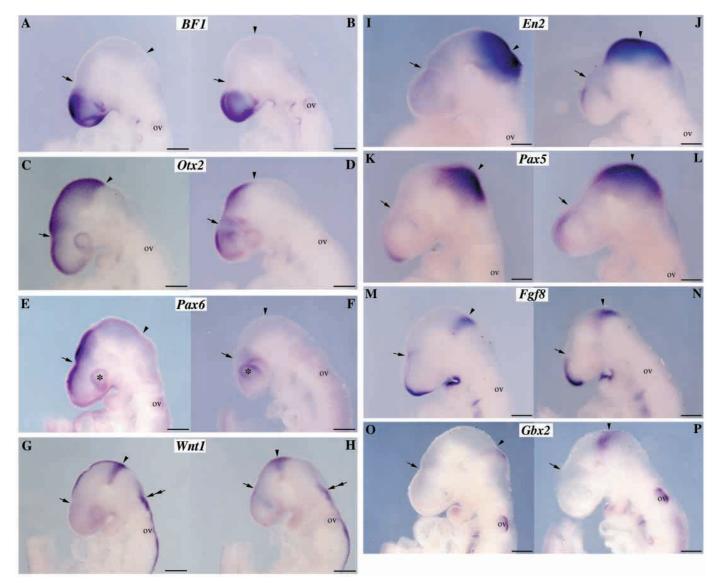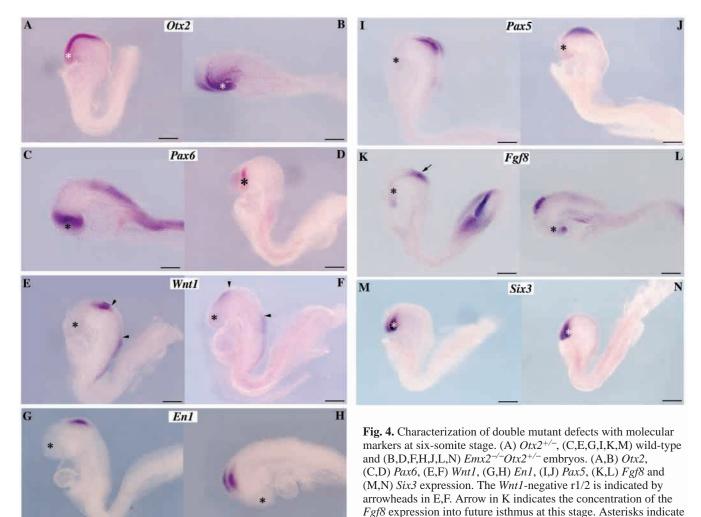
Fig. 3. Characterization of double mutant defects with molecular markers at 9.5 dpc. (A,E,G,I,K,M,O) Wild-type, (C) *Otx2*$^{+/-}$ and (B,D,F,H,J,L,N,P) *Emx2*$^{-/-}$*Otx2*$^{+/-}$ embryos. (A,B) *BF1,* (C,D) *Otx2*, (E,F) *Pax6*, (G,H) *Wnt1*, (I,J) *En2*, (K,L) *Pax5*, (M,N) *Fgf8* and (O,P) *Gbx2* expression. Arrows and arrowheads indicate the positions of the telodiencephalicus and isthmus, respectively. Double arrows in G,H indicate the anterior terminus (r3) of *Wnt1* expression in the roof of spinal cord, and asterisks in E,F denote eyes. ov, otic vesicle. Scale bars: 250 μm.

Miyamoto et al., 1997). The F$_5$ and F$_3$ generations of *Otx2* and *Emx2* heterozygotes, respectively, were the source for the present analysis.

Double heterozygotes (*Emx2*$^{+/-}$*Otx2*$^{+/-}$) were obtained at Mendelian ratio by crosses between *Emx2*$^{+/-}$ and *Otx2*$^{+/-}$ single heterozygotes. These double heterozygotes were subsequently mated with *Emx2*$^{+/-}$ single heterozygotes so as to generate *Emx2*$^{-/-}$ homozygous and *Otx2*$^{+/-}$ heterozygous (*Emx2*$^{-/-}$*Otx2*$^{+/-}$) double mutants (hereafter referred to as double mutants). The double mutants were obtained at Mendelian ratio at 15.5 dpc; however, none survived beyond 16.5 dpc. Morphologically, defects were not apparent in *Otx2*$^{+/-}$ mutants of this pedigree (Matsuo et al., 1995; Fig. 1). *Emx2*$^{-/-}$ mutants exhibited defects solely in the medial pallium, as previously reported (Yoshida et al., 1997; Fig. 1). *Emx2*$^{+/-}$*Otx2*$^{+/-}$ double heterozygotes displayed defects in

forebrain structures similar to, but significantly milder than, *Emx2*$^{-/-}$*Otx2*$^{+/-}$ double mutants.

The 15.5 dpc *Emx2*$^{-/-}$*Otx2*$^{+/-}$ double mutant brain demonstrated severe defects in the dorsal forebrain (Fig. 1A-H). In the telencephalon, cerebral hemispheres were present, but greatly diminished. The medial region of the cerebral cortex, which juxtaposes to the choroidal roof, is normally the territory of archicortex structures, i.e. the hippocampus (the dentate gyrus and CA fields) and para-hippocampal subicular cortex. The choroidal roof was expanded in the double mutants. Furthermore, no histological signs denoting archipallium structures could be identified; the defects were substantially more severe than those in *Emx2*$^{-/-}$ single mutants (Yoshida et al., 1997; Fig. 1). The choroid plexus did not develop in the third ventricle. In the cerebral cortex that was present laterally, no axonal fasciculation of the corpus callosum, anterior

Fig. 4. Characterization of double mutant defects with molecular markers at six-somite stage. (A) $Otx2^{+/-}$, (C,E,G,I,K,M) wild-type and (B,D,F,H,J,L,N) $Emx2^{-/-}Otx2^{+/-}$ embryos. (A,B) $Otx2$, (C,D) $Pax6$, (E,F) $Wnt1$, (G,H) $En1$, (I,J) $Pax5$, (K,L) $Fgf8$ and (M,N) $Six3$ expression. The $Wnt1$-negative r1/2 is indicated by arrowheads in E,F. Arrow in K indicates the concentration of the $Fgf8$ expression into future isthmus at this stage. Asterisks indicate the optic cup. Scale bars: 150 μm.

commissure, fornix or fimbria was in evidence. Cortical layers were poorly differentiated and laminar organization was not apparent; that is, the cortical plate was thin and sparse, and boundaries between the cortical plate and other layers could not be distinguished (data not shown). Defects were not observed in anterior structures, including the septum, but lateral and medial ganglionic eminences were hyperplastic.

The dorsal and ventral thalamus and pretectum were not apparent in $Emx2^{-/-}Otx2^{+/-}$ double mutants. The hypothalamus, mammillary region and hypophysis were relatively normal. The neurohypophysis was normal, but the adenohypophysis was irregularly shaped (data not shown). Zlth, which divides the ventral and dorsal thalamus, or the habenulopeduncular tract separating the pretectum and dorsal thalamus, were not observed in the double mutants. The posterior commissure typically occurs between the pretectum and tectum. The commissure was located proximal to the sulcus telodiencephalicus in the double mutants (Fig. 1D); moreover, only traces of structures that may have corresponded to the posterior pretectum were evident. The posterior commissure was reduced in size and poorly fasciculated. Additionally, the anterior boundary of the mesencephalon was poorly differentiated. The tectum was greatly enlarged occupying the original epithalamus and pretectum regions; in

this midbrain, the darkly stained ventricular proliferating field was expanded, whereas the differentiating field was narrowed. The tegmentum developed normally.

Histological analysis was subsequently conducted at 12.5 dpc upon near completion of rapid cell proliferation in the telencephalon. In $Emx2^{-/-}Otx2^{+/-}$ double mutants, the telencephalon was small and diminished, particularly in the dorsomedial aspect (Fig. 1I-L). Consequently, the telencephalic roof was enlarged and exposed. Evagination of the medial telencephalic pallium beyond the sulcus telodiencephalicus was poor and the hippocampal region did not develop in the double mutants (Fig. 1M-P). Ganglionic eminence and the mesencephalon were not hyperplastic at this stage. Neither the ventral nor dorsal thalamus was apparent; however, a commissural structure was present that may have corresponded to the posterior pretectum. Ventral structures, possibly corresponding to the hypothalamus, mammillary region and tegmentum, were evident. Isthmic constriction was observed, however, it was shifted rostrally (Fig. 1P).

Wild-type olfactory bulb primordium exhibits mitral and tufted cell layers at 12.5 dpc. The double mutants displayed a very small olfactory bulb that lacked the layered structure. Histologically tufted cells were present, but mitral cell layers were not (data not shown). Olfactory neurons did not project

to the olfactory bulb; rather, the nerve fivers were tangled outside the bulb. Several defects also occurred in the eyes. Lenses were irregularly shaped and the outer/inner layers of the retina were hyperplastic (data not shown). Consequently, *Otx2* and *Emx2* appear to cooperate in several steps of forebrain development. These genes interact in corticogenesis,
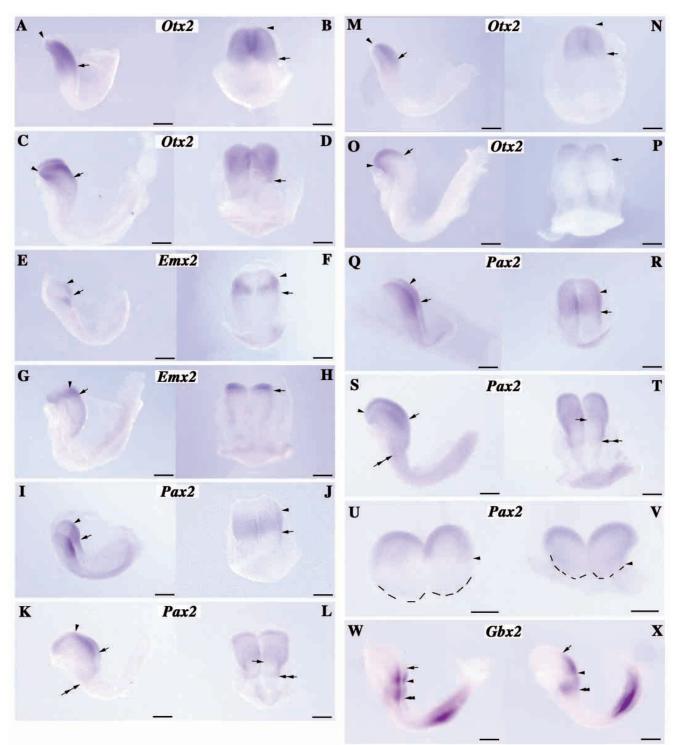

Fig. 5. Onset of double mutant defects. (A-D,M-P) *Otx2*, (E-H) *Emx2*, (I-L,Q-V) *Pax2* and *Gbx2* (W,X) expression at the three-(A,B,E,F,I,J,M,N,Q,R) and four- (C,D,G,H,K,L,O,P,S-X) somite stages. (A-L,U,W) Wild-type embryos and (M-T,V,X) *Emx2⁻ᐟ⁻Otx2⁺ᐟ⁻* embryos. (A,C,E,G,I,K,M,O,Q,S,W,X) Lateral views; (B,D,F,H,J,L,N,P,R,T) dorsal views; and (U,V) frontal views. Arrows denote the posterior limit and arrowheads the anterior limit of expressions. In S,T, arrows and double arrows indicate the posterior limits of expression in the most medial (future ventral) and lateral (future dorsal) points, respectively; the double arrows coincide with preotic sulcus. Broken lines in U,V indicate the anterior end of the neural plate. In W,X, arrows indicate the anterior limit of the expression, single arrowheads preotic sulcus and double arrowheads otic sulcus. Scale bars: 150 μm.
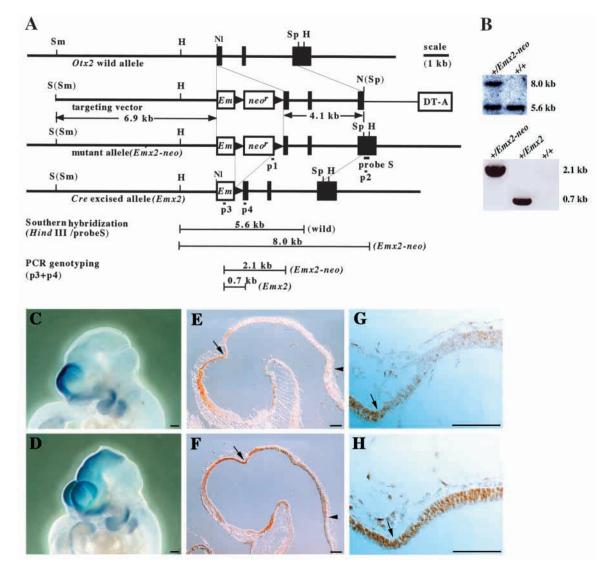
Fig. 6. Targeted knock-in of *Emx2* cDNA into the *Otx2* locus. (A) Diagrammatic representation of knock-in strategy. Thick lines represent *Otx2* genomic sequences; thin lines, pBluescript sequences; black boxes, *Otx2* coding exons; black triangles, *loxP* sequences. White boxes denoted as *Em*, *neo^r* and DT-A indicate *Emx2* cDNA lacking 3′UTR, neomycin-resistant gene lacking polyadenylation signal driven by *Pgk1* promoter and diphtheria toxin-A fragment gene with MCI promoter, respectively. S is the probe for Southern blotting used to identify homologous recombinant ES cells shown in B; p1 and p2 are PCR primers used in the detection of the homologous recombinants in ES cells, and p3 and p4 are PCR primers used in the detection of the deletion of the *neo^r* cassette in F$_1$ heterozygotes. H, *Hind*III; N, *Not*I; Nl, *Nla*III; S, *Sal*I; Sm, *Sma*I; Sp, *Sph*I. (B) The top panel displays an example of Southern blotting used to identify homologous recombinants in ES cells; the bottom panel displays an example of the PCR genotyping for the deletion of *neo^r* cassette in F$_1$ offspring obtained by mating between male chimera and *Cre* females. (C,D) RNA expressions from both endogenous and knocked-in *Emx2* at 10.5 dpc in a wild-type embryo (C) and a knock-in mutant (D). *Emx2* is expressed in the caudal diencephalon and mesencephalon where endogenous *Emx2* is absent. (E,F) EMX2 protein expressions at 10.5 dpc in a wild-type (E) and a knock-in embryo (F). Consistent with the ectopic mRNA expression, EMX2 protein is detected in the caudal diencephalon and mesencephalon. The endogenous *Otx2* expression and thus the knocked-in *Emx2* expression is somewhat weaker in the midbrain than in the forebrain at this stage. (G,H) Enlarged views of E,F (respectively) at the telodiencephalicus level indicated by arrows. Arrowheads indicate the isthmus. Scale bars: 125 μm.
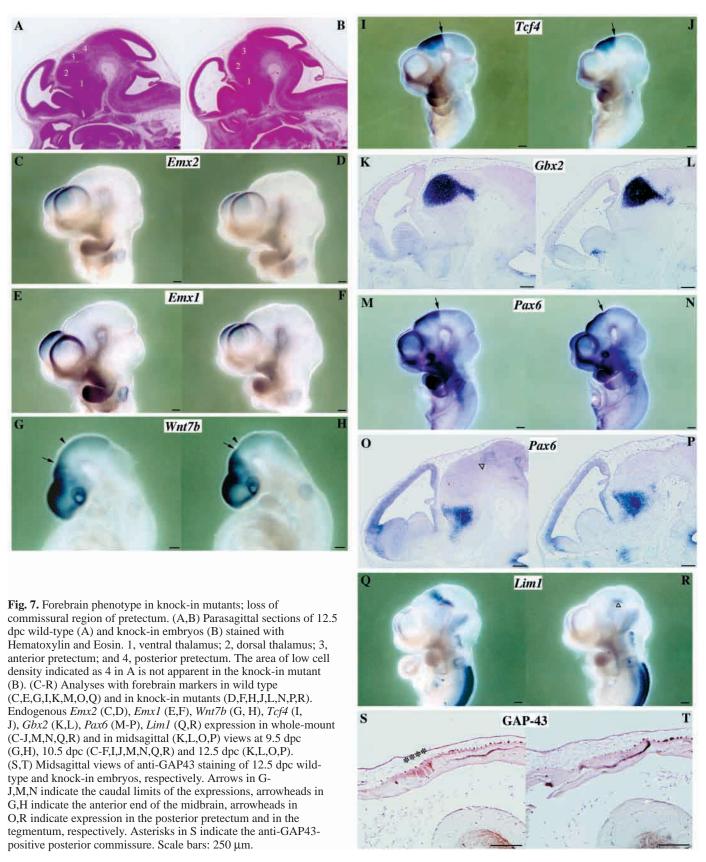
archipallium/roof development and the formation of sensory organs, the details of which will be reported elsewhere. This study focuses on the roles of *Emx2* and *Otx2* in diencephalon development.

Molecular characterization of diencephalic defects

At 11.5 dpc, several genes are expressed region specifically in the diencephalon. Affected structures were confirmed with these molecular markers; expression of each marker used is

schematically summarized in Fig. 9B. *Tcf4* is strongly expressed in the dorsal thalamus and pretectum, whereas expression in the ventral thalamus is weak (Fig. 2A; Cho and Dressler, 1998; Korinek et al., 1998). The double mutants lost the *Tcf4*-weak ventral thalamus and the majority of *Tcf4*-intense structures (Fig. 2B); however, traces of structures displaying intense *Tcf4* expression were in evidence. The posterior commissure, which originates from the posterior pretectum (Mastick et al., 1997), developed in the double

mutants. Consequently, this *Tcf4*-positive structure in the double mutants most probably corresponds to the posterior pretectum. The posterior pretectum normally expresses *Lim1*

(Barnes et al., 1994; Fujii et al., 1994; Mastick et al., 1997). Indeed, *Lim1* expression was typically present in the double mutants (Fig. 2C,D). Wild-type embryos display *Dlx1*

Fig. 7. Forebrain phenotype in knock-in mutants; loss of commissural region of pretectum. (A,B) Parasagittal sections of 12.5 dpc wild-type (A) and knock-in embryos (B) stained with Hematoxylin and Eosin. 1, ventral thalamus; 2, dorsal thalamus; 3, anterior pretectum; and 4, posterior pretectum. The area of low cell density indicated as 4 in A is not apparent in the knock-in mutant (B). (C-R) Analyses with forebrain markers in wild type (C,E,G,I,K,M,O,Q) and in knock-in mutants (D,F,H,J,L,N,P,R). Endogenous *Emx2* (C,D), *Emx1* (E,F), *Wnt7b* (G, H), *Tcf4* (I, J), *Gbx2* (K,L), *Pax6* (M-P), *Lim1* (Q,R) expression in whole-mount (C-J,M,N,Q,R) and in midsagittal (K,L,O,P) views at 9.5 dpc (G,H), 10.5 dpc (C-F,I,J,M,N,Q,R) and 12.5 dpc (K,L,O,P). (S,T) Midsagittal views of anti-GAP43 staining of 12.5 dpc wild-type and knock-in embryos, respectively. Arrows in G-J,M,N indicate the caudal limits of the expressions, arrowheads in G,H indicate the anterior end of the midbrain, arrowheads in O,R indicate expression in the posterior pretectum and in the tegmentum, respectively. Asterisks in S indicate the anti-GAP43-positive posterior commissure. Scale bars: 250 μm.

expression in the ventral thalamus, entopedunucular area, hypothalamic cell cord and ganglionic eminence (Fig. 2E; Bulfone et al., 1993; Eisenstat et al., 1999). *Dlx1*-positive ganglionic eminence, hypothalamic cell cord and entopedunucular area were present in the double mutants; however, the ventral thalamus was absent (Fig. 2F), as indicated by *Tcf4* expression. *Gbx2* is expressed in the dorsal thalamus and ganglionic eminence (Fig. 2G; Bulfone et al., 1993). Expression was present in the ganglionic eminence; however, *Gbx2*-positive dorsal thalamus was absent in the double mutants (Fig. 2H). *Ebf1* is expressed in the anterior pretectum, anterior tectum and tegmentum (Fig. 2I; Garel et al., 1997). Double mutants exhibited the expression in the anterior tectum and tegmentum, but these mutants lacked *Ebf1*-positive anterior pretectum (Fig. 2J).

Pax6 is expressed in the telencephalon and diencephalon. At 11.5 dpc, it is strong in the ventral thalamus, posterior pretectum and tegmentum (Fig. 2K; Walther and Gruss, 1991). The strong expression in the basal posterior pretectum and midbrain tegmentum was retained, but all other *Pax6* expression was lost in the double mutants (Fig. 2L). *Otx1* is expressed spanning the telencephalon, diencephalon and mesencephalon. The most intense *Otx1* expression is observed in the anterior pretectum, tegmentum and a boundary region along zlth (Fig. 2M; Simeone et al., 1993; Boncinelli et al., 1993). Double mutants lacked the *Otx1*-rich anterior pretectum and zlth region (Fig. 2N).

Morphologically, the mesencephalon was normal in the 12.5 dpc double mutants. It is possible, however, that the diencephalic defects affected rostrocaudal regionalization in the mesencephalon. *Mek4* is expressed in a gradient in wild-type embryos. High levels of *Mek4* occur in the anterior tectum, whereas low levels occur caudally (Fig. 2O; Cheng and Flanagan, 1994). In contrast, *ephrin-A2* expression is high in caudal mesencephalon and low in anterior mesencephalon (Fig. 2Q; Flenniken et al., 1996; Feldheim et al., 1998; Feldheim et al., 2000). The double mutants exhibited normal patterns for *Mek4* and *ephrin-A2* expression (Fig. 2P,R).

Marker analyses, in concert with morphological features, indicate that the precommissural region of the pretectum and dorsal and ventral thalamus do not develop in double mutants. The commissural region of the pretectum and the ventral structures were present, including the hypothalamus, mammillary region and tegmentum.

Molecular characterization of defects at earlier stages

No diencephalic structures are subdivided morphologically at 9.5 dpc; nor are any region-specific molecular markers expressed in the diencephalon. At this stage, telencephalic vesicle formation begins and *BF1* is expressed throughout the entire telencephalic neuroepithelium with the exceptions of the most medial and caudal regions adjacent to the choroidal roof and diencephalon (Tao and Lai, 1992). In the 9.5 dpc double mutants, the *BF1*-positive region was largely normal (Fig. 3A,B). Normally *Otx2* is expressed in the forebrain and midbrain with the caudal limit at the mid/hindbrain junction (Simeone et al., 1993; Matsuo et al., 1995). In comparison with *Otx2*$^{+/-}$ single heterozygotes, *Otx2* expression from the remaining allele was greatly reduced in *Emx2*$^{-/-}$*Otx2*$^{+/-}$
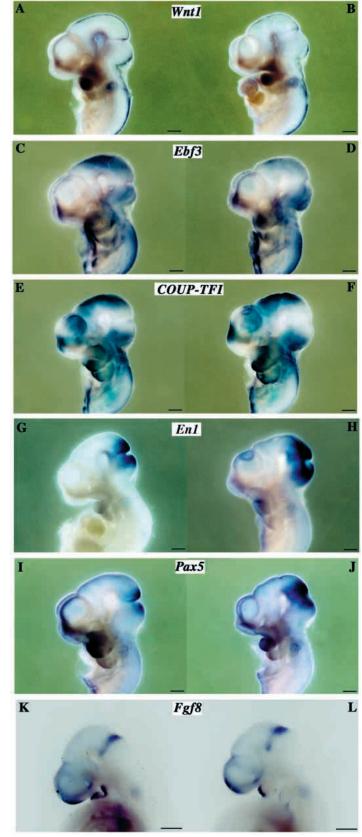

Fig. 8. Midbrain phenotype in knock-in mutants. (A,C,E,G,I,K) Wild-type and (B,D,F,H,J,L) knock-in mutant embryos. (A,B) *Wnt1*, (C,D) *Ebf3*, (E,F) *COUP-TFI*, (G,H) *En1*, (I,J) *Pax5* and (K,L) *Fgf8* expression at 9.5 dpc (K,L) and 10.5 dpc (A-J). Scale bars: 125 μm.

double mutants, particularly in the region caudal to the sulcus telodiencephalicus (Fig. 3C,D). The caudal limit shifted rostrally and expression was restricted to the more dorsal region.

Pax6 expression is found over the telencephalon and diencephalon at 9.5 dpc in wild-type embryos (Fig. 3E; Walther and Gruss, 1991; Stoykova et al., 1996). *Pax6* expression was scarcely observed in double mutants, however, its expression in the eyes was retained (Fig. 3F). *Wnt7b* expression was present in the double mutant telencephalon, but the mutants lost a *Wnt7b*-positive diencephalon (data not shown, compare Fig. 3F with Fig. 7G). *Fgf8* expression in the anterior neural ridge was normally present, but the roof at the position of the telodiencephalicus or the roof of ventral thalamus was absent (Fig. 3M,N).

Wnt1 is expressed in the dorsal midline over the caudal diencephalon and mesencephalon, and in a characteristic lateral stripe at the isthmus in 9.5 dpc wild-type embryos (Fig. 3G; Parr et al., 1993). Double mutants demonstrated a reduced *Wnt1*-positive region in the roof as well as a decrease in the level of *Wnt1* expression laterally. The isthmic stripe was formed, but it was shifted rostrally. In wild-type embryos, caudally to the isthmus, the anterior metencephalon, r1 and r2, does not express *Wnt1* (Fig. 3G; McMahon et al., 1992; Echelard et al., 1994). This *Wnt1*-negative region was expanded in the double mutants (Fig. 3H).

En2 is expressed in a gradient over the caudal mesencephalon and r1 at 9.5 dpc in wild-type embryos (Fig. 3I; Davis and Joyner, 1988; Davis et al., 1988). The double mutants exhibited expanded *En2* expression rostral to the isthmic constriction, and the gradient is less distinct (Fig. 3J). Concomitantly, the region between the anterior terminus of *En2* expression and the sulcus telodiencephalicus was greatly diminished. Moreover, the *En2*-positive region caudal to the isthmic constriction and the region between the posterior terminus of *En2* expression and the otic vesicle appeared enlarged. Normally *Pax5* is also expressed in the mesencephalon and r1 (Fig. 3K; Asano and Gruss, 1992; Urbanek et al., 1994). The *Pax5*-positive region both rostral and caudal to the isthmic constriction was enlarged, while the negative region extending up to the sulcus telodiencephalicus was greatly reduced in double mutants (Fig. 3L). The region between the caudal end of *Pax5* expression and the otic vesicle appeared enlarged. Isthmus also expresses *Fgf8* and *Gbx2* (Fig. 3M,O; Bulfone et al., 1993; Crossley and Martin, 1995; Mahmood et al., 1995). These expressions were shifted anteriorly in the double mutants (Fig. 3N,P). In addition, the distance between the *Fgf8*- and *Gbx2*-positive isthmic stripe and otic vesicles appeared increased by the double mutation.

Marker analyses at 9.5 dpc are consistent with the defects at 11.5 dpc. Telencephalon and mesencephalon formation is fairly normal; however, the major region of the diencephalon does not develop and *Pax6* expression in the forebrain is lost in *Emx2⁻/⁻Otx2⁺/⁻* mutants. Thus, the onset of the defects precedes this stage. The expansion of the anterior hindbrain was notable.

Onset of double mutant defects

Marker analyses were next performed at the six-somite stage, the point at which the initial brain regionalization is completed. The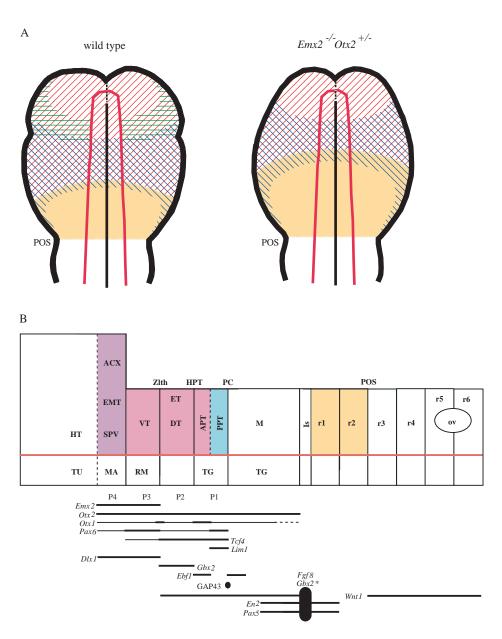 caudal limit of *Otx2* expression becomes distinct at the isthmus and the territory of the future forebrain and midbrain is established by this stage (Fig. 4A; Acampora et al., 1995; Rubenstein and Shimamura, 1998). Double mutants displayed a greatly reduced *Otx2*-positive region (Fig. 4B). *Pax6* expression normally occurs in the forebrain, as well as in the laterocaudal component of the incipient optic cup, and the hindbrain and spinal cord (Fig. 4C; Walther and Gruss, 1991). *Pax6* expression was unchanged in the hindbrain and spinal cord, and remained evident in the optic cup in double mutants (Fig. 4D); however, it was scarcely observed in the forebrain.

The *Wnt1* expression was already reduced and shifted anteriorly in the double mutants at the six-somite stage (Fig. 4E,F; McMahon et al., 1992; Bally-Cuif et al., 1995). In addition, the *Wnt1*-negative anterior hindbrain, corresponding to future r1 and r2, exhibited expansion. In wild-type brain, the *En1*- and *Pax5*-positive regions, which initially cover the entire prospective mesencephalon (compare with Fig. 8G,I), have completed regression to the caudal portion by this stage (Fig. 4G,I; Joyner, 1996). Double mutants demonstrated somewhat expansion of the positive domains accompanied by an anterior shift (Fig. 4H,J). *Fgf8* expression in the midbrain-hindbrain boundary in wild-type embryos begins to be confined to the future isthmus at the six-somite stage (Fig. 4K; Suda et al., 1997). However, this event was less distinct in the double mutants (Fig. 4L). *Six3* expression is observed in the most rostral neuroectoderm at the six-somite stage in wild-type embryos (Fig. 4M; Oliver et al., 1995). Double mutants exhibited normal *Six3* expression (Fig. 4M,N). Consequently, the diencephalon corresponding to the future ventral thalamus, dorsal thalamus and anterior pretectum is probably already lost at this point. Additionally, anterior hindbrain expansion, the loss of *Pax6* expression, reductions in *Otx2* and *Wnt1* expression, and the elevation of *En1* and *Pax5* expression were also evident at the six-somite stage in *Emx2⁻/⁻Otx2⁺/⁻* mutants.

Otx2 is expressed in the anterior neuroectoderm from the earliest stage of its induction (Fig. 5A-D; Acampora et al., 1995). As a result, the onset of the double mutant defects should closely correlate with the onset of *Emx2* expression. *Emx2* was not detectable at the two-somite stage, but at the three-somite stage, it occurred in the laterocaudal forebrain primordia (Fig. 5E,F). This *Emx2* expression increases and expands rostrally to the future dorsal aspect by the five-somite stage (Fig. 5G,H; Shimamura et al., 1997). *Pax2* expression, which corresponds to the future midbrain, also occurs around the three-somite stage in the caudal portion of the *Otx2*-positive region (Fig. 5I,J; Rowitch and McMahon, 1995). At this stage, the anterior limit of *Pax2* expression appears to overlap with the posterior limit of *Emx2* expression; moreover, its caudal limit extends beyond the caudal limit of *Otx2* expression. At the four-somite stage, *Pax2* expression extends caudally into the preotic sulcus at the most lateral (future dorsal) edge; however, in the medial (future lateral and ventral) region, expression terminates more rostrally (Fig. 5K,L). This laterally *Pax2*-positive and medially *Pax2*-negative region corresponds to future r1 and/or r2. *Gbx2* is expressed in this preotic as well as the otic region at the 3-4 somite stage (Fig. 5W). *Pax6* expression occurs at the four-somite stage, and its caudal limit nearly coincides with the caudal limit of *Emx2* expression (Shimamura et al., 1997; Inoue et al., 2000).

The defect was evident at the three-somite stage upon evaluation of the double mutant phenotype via *Otx2* expression

Fig. 9. An interpretation of *Emx2⁻/⁻Otx2⁺/⁻* double and *Otx2⁺/ᴱᵐˣ²* knock-in mutant defects. (A) The onset of double mutant defects at the four-somite stage. *Emx2*-positive domain shown in green horizontal lines was lost in the double mutants. Consequently *Otx2*-positive region shown in red oblique lines was reduced both rostrocaudally and lateromedially. Moreover, the *Pax2*-positive area shown in blue oblique lines shifted rostrally, resulting in the reduction of anterior *Otx2*-positive and *Pax2*-negative area. Concomitantly *Gbx2*-positive area rostral to preotic sulcus (POS), painted in yellow, expanded. (B) A prosomeric view of affected region in double and knock-in mutants. P3 ventral thalamus, P2 dorsal thalamus and rostral P1 anterior pretectum (shown in red) were lost by the defects at the three- to four-somite stage in double mutants. P4 archipallium shown in purple was probably also lost by the defects at the same stage, though no detailed analysis was conducted in the present study. The r1 and r2 shown in yellow expand to compensate for the loss of the anterior structures in the double mutants. Posterior pretectum shown in blue develops in double mutants, but is specifically lost in knock-in mutants. *Emx2, Otx2, Otx1, Pax6, Tcf4, Lim1, Dlx1, Gbx2, Ebf1* and GAP43 give their dorsal expression at 11.5dpc. Intense and weak expression are shown by thick and thin lines, respectively, in *Otx1, Pax6* and *Tcf4. Fgf8, Gbx2, Wnt1, En2* and *Pax5* give the expression at 9.5 dpc. ACX, archicortex; APT, anterior pretectum; DT, dorsal thalamus; EMT, eminentia thalami; ET, epithalamus; HPT, habenulopeduncular tract; HT, hypothalamus; Is, isthmus; M, midbrain; MA, mammillary area; ov, otic vesicle; PC, posterior commissure; POS, preotic sulcus; PPT, posterior pretectum; RM, retro mammillary area; SPV, suprapreoptic paraventricular area; TG, tegmentum; TU, tuberal hypothalamus; VT, ventral thalamus; Zlth, zonalimitans interthalamica. Red lines indicate the boundary between alar and basal plates.

(Fig. 5M,N). The *Otx2*-positive domain was reduced both rostrocaudally and lateromedially (future dorsoventrally). The rostrocaudal reduction of the *Otx2*-positive domain was more apparent at the four-somite stage (Fig. 5O,P). *Pax2* expression was more diffuse and expanded rostrally in double mutants at the three-somite stage (Fig. 5Q,R). At the four-somite stage, the caudal limit of *Pax2* expression in the medial region had shifted rostrally. Furthermore, the laterally *Pax2*-positive and medially *Pax2*-negative region had expanded (Fig. 5S,T), and the anterior *Pax2*-negative domain was greatly reduced (Fig. 5U,V). Concomitantly, the anterior limit of the *Gbx2* expression in the preotic region shifted rostrally (Fig. 5X). Thus, it appears most likely that the *Emx2*-positive domain failed to develop, the *Pax2*-positive domain underwent a rostral shift and the *Gbx2*-positive region anterior to preotic sulcus

expanded by the four-somite stage in the *Emx2⁻/⁻Otx2⁺/⁻* double mutants (see Fig. 9A). *Wnt1* expression was faint, whereas *Pax6* expression was not detected in double mutants at the four-somite stage as in later stages (data not shown).

Ectopic *Emx2* expression in *Emx2*-negative diencephalon and mesencephalon

At 10.5 dpc, *Emx2* is typically expressed rostrally to zlth. *Emx2* expression is not observed in the dorsal thalamus, pretectum or tectum (Simeone et al., 1992a; Shimamura, et al., 1997; Yoshida et al., 1997). *Emx2* functions in the development of diencephalic structures were also examined by its ectopic expression in these endogenously *Emx2*-negative regions under the *Otx2* heterozygous state. For this purpose the *Otx2* gene was replaced with Emx2 cDNA by homologous recombination

in TT2 ES cells, as described in Fig. 6A. The *neo*-resistant gene directed by the phosphoglycerate kinase 1 (*Pgk1*) promoter for the selection of the recombinants was flanked with *loxP* sequences. To exclude possible effects of the *Pgk1* promoter on the *Otx2* transcriptional machinery, the gene was deleted by crossing chimeras derived from the homologous recombinants with transgenic females expressing Cre in their zygotes (Fig. 6B; Sakai and Miyazaki, 1997). F_2 embryos derived from these F_1 heterozygotes ($Otx2^{+/Emx2}$) expressed *Emx2* in the dorsal thalamus, pretectum and tectum, as expected (Fig. 6C-H).

The ventral and dorsal thalamus, tectum, hypothalamus, mammillary region and tegmentum were morphologically normal in these 12.5 dpc $Otx2^{+/Emx2}$ mutants (Fig. 7A,B). A structure similar to the precommissural region of the pretectum was also evident, but the commissural region of the pretectum was not apparent.

Endogenous *Emx2* and *Emx1* were expressed typically in the 10.5 dpc telencephalon of knock-in mutants (Fig. 7C-F; Simeone et al., 1992a; Yoshida et al., 1997). *Wnt7b* is normally expressed in the 9.5 dpc forebrain, however, expression does not occur in its most posterior aspect (Fig. 7G; Parr et al., 1993). This *Wnt7b*-negative caudal diencephalon was nearly lost in knock-in mutants (Fig. 7H). *Tcf4*-intense diencephalon existed in the 10.5 dpc mutants; however, the domain was narrowed and its posterior aspect was not distinctly delineated, as in wild-type embryos (Fig. 7I,J). *Gbx2*-positive dorsal thalamus and *Ebf1*-positive anterior pretectum and anterior tectum were present despite the lack of a *Ebf1*-negative posterior pretectum in the 12.5 dpc knock-in mutants (Fig. 7K,L; data not shown; compare with Fig. 2I). *Pax6* expression in the 10.5 dpc forebrain was largely normal, although its caudal-most expression, typically corresponding to the posterior pretectum, was not sharply delineated (Fig. 7M,N). At 12.5 dpc, a *Pax6*-intense ventral thalamus was present, but the posterior pretectum was not observed (Fig. 7O,P). Ventral thalamus development was also confirmed with *Dlx1* (data not shown, compare with Fig. 2E). The *Lim1*-positive tegmentum was present, whereas the *Lim1*-positive posterior pretectum was not found in the 10.5 dpc knock-in mutants (Fig. 7Q,R). Anti-GAP43 antibody specifically detects the posterior commissure (Fig. 7S; Matsunaga et al., 2000). A GAP43-positive structure was not identified in 12.5 dpc $Otx2^{+/Emx2}$ mutants (Fig. 7T).

Among gene activity dorsally spanning the caudal diencephalon and mesencepalon, *Wnt1* and *Ebf3* (Garel et al., 1997) expression were decreased at 10.5 dpc (Fig. 8A-D). *COUP-TFI* expression (Qiu et al., 1994) was unchanged (Fig. 8E-F), whereas *En1* and *Pax5* expression was strongly enhanced (Fig. 8G-J). Knock-in mutants, however, displayed normal patterns of *Mek4* and *ephrin-A2* expression (data not shown; compare with Fig. 2O,Q). Isthmus formation typically occurs with normal *Fgf8* expression. *Fgf8* expression in the anterior neural ridge and the roof at the position of the telodiencephalicus was also normally present (Fig. 8K,L).

Marker analyses, in conjunction with morphological observations, indicate that the telencephalon, ventral and dorsal thalamus, anterior pretectum and mesencephalon developed in the knock-in mutants. However, the commissural region of the pretectum specifically failed to develop as a consequence of ectopic *Emx2* expression.

DISCUSSION

Emx2 cooperates with *Otx2* at the onset of its expression to generate the territory of the future diencephalon

In contrast to the hindbrain, the forebrain has long been thought not to possess neuromeric organization. However, a prosomeric model that postulates forebrain neuromeric organization has been presented on the basis of region-specific gene expression and other evidence. It is now generally believed to divide the caudal forebrain along the rostrocaudal axis into p1 pretectum, p2 dorsal thalamus/epithalamus and p3 ventral thalamus (Bulfone et al., 1993; Figdor and Stern, 1993; Puelles and Rubenstein, 1993; Rubenstein et al., 1994; Shimamura et al., 1995). Adjacent to the boundary between the tectum and p1 pretectum lies the posterior commissure; between p1 and p2 dorsal thalamus, the habenulopeduncular tract is found; between p2 and p3 ventral thalamus, the zona limitans interthalamica develops, respectively. The ventral and dorsal thalamus, epithalamus and anterior pretectum were lost in $Emx2^{-/-}Otx2^{+/-}$ mutants (Fig. 9B). Consequently, *Emx2* and *Otx2* play crucial roles in diencephalon development. No other such genes are known.

Otx2 and *Emx2* are co-expressed in a variety of stages and sites during brain development. The double mutant defects at 15.5 dpc may reflect each of these *Otx2* and *Emx2* functions. Defects in the formation of the diencephalon, however, appear to reside within their functions at the three-somite stage when *Emx2* expression first occurs (Fig. 9). *Otx2* and *Gbx2* are among the genes known to be first expressed in the neuroectoderm. *Otx2* expression hallmarks the anterior neuroectoderm which corresponds to the future forebrain and midbrain. In contrast, *Gbx2* marks the posterior neuroectoderm (Wassarman et al., 1997); at the three- to four-somite stage its expression is found in preotic and otic regions. *Pax2* and *En1* expression occurs nearly simultaneously at the three-somite stage in the entire prospective midbrain (Rowitch and McMahon, 1995), probably as a result of signals such as *Fgf4* from the anterior notochord (Shamim et al., 1999). Their rostral limits likely overlap with *Emx2* expression. *Wnt1* expression begins at this stage in a similar manner with respect to *En1* (Bally-Cuif et al., 1995). Onset of *Pax6* expression is somewhat late around the four-somite stage. Moreover, the caudal limits of *Pax6* and *Emx2* expression appear to coincide with one another at this stage (Shimamura et al., 1997; Inoue et al., 2000).

At the three-somite stage, double mutants displayed an *Otx2*-positive region which was reduced rostrocaudally. Additionally, the *Pax2*-positive domain was diffuse and extended in a rostral manner. By the four-somite stage, the anterior *Pax2*-negative region was reduced, whereas the caudal limit of *Pax2* and the anterior limit of the *Gbx2* expression shifted rostrally; the *Gbx2*-positive region rostral to preotic sulcus expanded (Fig. 9A). It is quite simple to interpret the phenotype as a consequence of the loss of the *Emx2*-positive domain in double mutants and the shift of the *Pax2*-positive domain to the anterior *Otx2*-positive/*Emx2*-negative domain.

Pax6 expression was not induced in double mutants. Apparently, *Emx2* and *Otx2* are located upstream of *Pax6* in development of the diencephalon. *Sey* mutants, which possess a null mutation in the *Pax6* gene, suggested that *Pax6* is

important for correct dorsoventral and anteroposterior patterning in the diencephalon (Grindley et al., 1997; Stoykova et al., 1997; Warren and Price, 1997). Each region of the diencephalon, ventral thalamus, dorsal thalamus and pretectum, however, emerges in *sey/sey* mutants. Consequently, *Emx2* and *Otx2* regulate other genes with respect to diencephalon development. *Wnt1* expression also decreased at the initial stage in double mutants. *Emx*-binding sites exist in the *cis* regulatory region of the *Wnt1* gene (Iler et al., 1995). Wingless and engrailed are hypothesized to be targets of the head gap genes *otd* and *ems* in *Drosophila* (Royet and Finkelstein, 1995). However, *Wnt1* mutants as well as *En1* and *En2* mutants develop diencephalic structures (Joyner et al., 1991; McMahon et al., 1992; Millen et al., 1994; Wurst et al., 1994).

The 15.5 dpc defects in the neocortex are apparently due to later *Emx2* and *Otx2* functions in corticogenesis, as suggested by *BF1* expression at 9.5 dpc; however failure of archipallium formation in the double mutants may also reside within the *Emx2* functions at the three-somite stage (Fig. 9). In the prosomeric model, the archipallium belongs to the p4 structures anterior to p3 ventral thalamus (Rubenstein et al., 1998). Wild-type embryos demonstrate a rostral extension of the lateral (future dorsal) portion of the anterior-most *Emx2*-positive region (Fig. 5C,D; Fig. 9A). This extension may include the presumptive dorsomedial region of the forebrain or archipallium (Rubenstein and Shimamura, 1998). The *Otx2*-positive region was reduced not only rostrocaudally but also lateromedially (future dorsoventrally) in double mutants at the three-somite stage (Fig. 5G,H; Fig. 9B). The detailed analysis of archipallium defects in double mutants will be reported elsewhere.

Does the neuroectoderm anterior to the preotic sulcus constitute a unit?

The expansion of the anterior hindbrain in 9.5 dpc *Emx2$^{-/-}$Otx2$^{+/-}$* double mutants is puzzling. The region between the otic vesicle and isthmus, indicated by *Fgf8* and *Gbx2* expression, appeared expanded. The region between the otic vesicle and the caudal terminus of *En2* and *Pax5* expression was enlarged; their expression in r1 was also expanded. The *Wnt1*-negative region in the anterior hindbrain increased at 9.5 dpc and the six-somite stage. Consequently the expanded region may correspond to r1 and r2. The r1/2 also enlarges in *Otx1$^{+/-}$Otx2$^{+/-}$* double heterozygotes that fail to develop a midbrain (Suda et al., 1997). We speculated that suppressive signals originating within the midbrain might be necessary for correct r1/2 development; however, such signals from the diencephalon are very unlikely.

Of note is the expansion of the laterally *Pax2*-positive (but medially *Pax2*-negative region) or the *Gbx2*-positive region anterior to the preotic sulcus in double mutants at the four-somite stage (Fig. 5S,T,X; Fig. 9). This event is most probably brought about by the loss of the *Emx2*-positive region and anterior shift of *Pax2*-positive region. Morphologically, the anterior neuroectoderm is initially demarcated by the preotic sulcus, which is apparent around the three-somite stage and includes future r1 and r2. Unfortunately, no molecular markers are available specific to the prospective r1/2 territory at early stages. As a result, more detailed analyses are necessary in future studies in order to determine the direct correlation of

the defect at the four-somite stage with r1/2 expansion at 9.5 dpc.

The loss of anterior hindbrain in *Gbx2*-null mutants accompanies a posterior expansion of the *Otx2*-positive midbrain (Wassarman et al., 1997; Miller et al., 1999). *En1*, *En2*, *Pax2*, *Pax5* or *Wnt1* mutants fail to develop midbrain without expansion of r1/2. These midbrain genes, however, may function in midbrain development after the establishment of its territory (McMahon et al., 1992; Schwarz et al., 1999; Liu and Joyner, 2001). It is tempting to speculate that the region anterior to the preotic sulcus initially develops as a unit and that the anterior hindbrain expands to compensate when more anterior structures are lost before their subdivision into forebrain, midbrain and the anterior hindbrain. Clarification of the development of the preotic sulcus and r1/r2 might be important regarding investigations of rostral brain regionalization.

Emx2 and *Otx2* direct the development of the dorsal thalamus and anterior pretectum

The posterior limit of *Pax6* expression and the anterior limit of *En1* and *Pax2* expression are known to overlap at the six- to eight-somite stages in chicken. However, the expression of these genes segregates by the 10 somite stage (Matsunaga et al., 2000). The interaction between *Pax6*, *En1* and *Pax2* at this stage is believed to establish the boundary between the diencephalon and mesencephalon (Araki and Nakamura, 1999; Schwarz et al., 1999; Matsunaga et al., 2000). In the absence of *Pax6* expression, however, the posterior pretectum and tectum were regionalized in *Emx2$^{-/-}$Otx2$^{+/-}$* double mutants; the present study does not exclude the role of *Pax6* in the fine tuning of the boundary. After segregation from the *Pax6*-positive region, *En1*, *En2* and *Pax2* expression regress caudally (Dressler et al., 1990). At 10.5 dpc, the caudal limit of *Emx2* expression is in zlth (Simeone et al., 1992a; Shimamura et al., 1997), whereas that of *Pax6* occurs in the boundary between the diencephalon and mesencephalon (Walther and Gruss, 1995). *En1* and *En2*, and *Pax2* and *Pax5* are expressed in the caudal mesencephalon (Davis and Joyner, 1988; Dressler et al., 1990; Asano and Gruss, 1992; Millet et al., 1999). These observations raise the question of why the *Pax6*-positive, *Emx2*-negative anterior pretectum and dorsal thalamus are lost in *Emx2$^{-/-}$Otx2$^{+/-}$* double mutants.

A cell lineage analysis has revealed that restriction in cell movement between regions anterior and posterior to the presumptive zlth occurs immediately after the onset of *Pax6* expression at the four-somite stage (Inoue et al., 2000). At this juncture, the prospective pretectum and dorsal thalamus regions are diminutive. Consequently, two refined analyses are necessary to assess the origin of dorsal thalamus and pretectum cells. The caudal limit of *Emx2* expression must first be determined by expression analysis at the single cell level. This process will ascertain the distinction between its coincidence with the caudal limit of *Pax6* expression or the presence of *Emx2*-negative and *Pax6*-positive cells in this region already at the four-somite stage. The analysis should demonstrate the sequence of growth of the *Emx2*-negative, *Pax6*-positive diencephalon. Secondly, cell lineage analysis by genetic approach is necessary in order to determine the fate of *Emx2*-positive cells at the three- to four-somite stage. These studies are in progress; however, we speculate that the *Emx2*-positive

domain at the three-somite stage includes cells of the future dorsal thalamus and anterior pretectum, where *Emx2* expression is subsequently lost. Their development is compatible with *Emx2* expression as demonstrated by the $Otx2^{+/Emx2}$ knock-in mutation. Of course, it can not be excluded that a population of *Emx2*-negative and *Pax6*-positive cells at the four-somite stage generates the dorsal thalamus and anterior pretectum, depending on signals from *Emx2*-positive ventral thalamus.

Emx2 expression is not compatible with development of the commissural region of the pretectum

This study distinguished the developmental nature of the anterior and posterior pretectum. The anterior pretectum was lost in the double mutants, while the *Lim1*-positive commissural region of the pretectum developed (Fig. 9C). In contrast, formation of not only the entire endogenously *Emx2*-positive region, but also of the *Emx2*-negative dorsal thalamus, anterior pretectum and tectum, was compatible with ectopic *Emx2* expression by the $Otx2^{+/Emx2}$ knock-in mutation. Specifically, the development of the commissural region of the pretectum was not allowed by ectopic *Emx2* expression. Unfortunately, molecular markers for posterior pretectum were unavailable at earlier stages. As a result, analyses of defect onset is left to future investigations. The cellular origin of the posterior pretectum is the most significant aspect to be determined.

The tract of the posterior commissure forms just rostral to the caudal border of the *Pax6*-positive domain. Although few posterior commissure neurons express *Pax6* at 10.5 dpc, the point at which the posterior commissure can be identified, the neurons are thought to originate from *Pax6*-positive pretectum cells (Mastick et al., 1997). Schwartz et al. argue that *Pax6* is sufficient and necessary for the development of the commissure on the basis of its loss in their *sey/sey* mutants and its subsequent recovery by *Pax6*-transgenesis under a *Pax2* enhancer (Schwartz et al., 1999). *Pax6* expression was lost in $Emx2^{-/-}Otx2^{+/-}$ double mutants, however, the posterior commissure was present despite blurring. In the *sey/sey* mutants reported, the commissure was either completely absent (Stoykova et al., 1996; Warren and Price, 1997), lacking in dorsal axons (Mastick et al., 1997) or present but smaller than normal (Grindley et al., 1997).

Curiously, *Wnt1* expression decreased and *En1*, *En2*, *Pax2* and *Pax5* expression were enhanced by both double and knock-in mutations. However, the midbrain was normal in size at 12.5 dpc and displayed the normal rostrocaudal pattern of *Mek4* and *ephrin-A2* expression in both mutants. The anterior tectum developed as indicated by *Ebf1*, as well as *Mek4* expression. The causes and significance of changes in the expression of several midbrain genes, in conjunction with possible roles of the commissural region of the pretectum or diencephalon with respect to later midbrain development, including its hyperplasia at 15.5 dpc (Fig. 1), require further study.

Interaction between *Emx2* and *Otx2*

This study examined genetically the existence of interaction between *Emx2* and *Otx2* genes. It indicated that these two genes indeed interact in diencephalon development. *Otx1* also participates in diencephalon formation, as demonstrated by

Otx1/Otx2 double mutation (Acampora et al., 1997; Suda et al., 1997). Consequently *Otx2* interacts with both *Emx2* and *Otx1* in the development of the diencephalon. In addition, both *Emx2/Otx2* and *Otx1/Otx2* double mutants indicated the gene dose-dependent nature of the interactions between these genes. Each head subdomain appears to require differing *otd* and *ems* levels in *Drosophila* (Royet and Finkelstein, 1995). However, the question regarding the specifics of how *Emx2* interacts with *Otx2* remains unanswered. Both *Otx1* and *Otx2* gene products (OTX2 and OTX1) exhibit paired-like homeodomains; interaction between OTX2 and OTX1 through these homeodomains is probable. Furthermore, the homeodomains of *Emx1* and *Emx2* gene products (EMX1 and EMX2) belong to HEX class. The HEX homeodomain is too distant to allow homeodomain-homeodomain interactions with the paired-like homeodomains, however, our preliminary studies have suggested a direct protein-protein interaction between OTX2 and EMX2 proteins, possibly through homeodomain and non-homeodomain regions (Nakano et al., 2000). Alternatively, these genes might bind to each recognition site. Synergistic binding would activate the expression of common target genes.

The role of EMX2 in diencephalon development indicated by $Emx2^{-/-}Otx2^{+/-}$ double mutants, however, must reconcile with the fact that the diencephalon develops normally in $Emx2^{-/-}$ single mutants. *Otx2* expression is not restricted to the diencephalon. Several explanations are possible; however, it is quite simple to hypothesize that there exists a gene that complements *Emx2* and regulates diencephalon development through gene dose-dependent interactions with *Emx2*, *Otx2* and *Otx1*. *Emx1* would be a primary candidate for this unidentified gene. However, *Emx1* becomes expressed later at 9.5 dpc and not in the early diencephalon. Two genes, *Vax1* and *Vax2*, are also known that locate very closely to *Emx2* and *Emx1* genes in chromosomes 19 and 6, respectively. They possess similar homeodomains (Hallonet et al., 1998; Ohsaki et al., 1999), but their expression does not overlap with *Emx2* expression in the forebrain. Neither the *Emx1*, *Vax1* or *Vax2* gene was ectopically induced in the diencephalon of *Emx2* single mutants at the four-somite stage (data not shown). The *Not* class of genes also exhibits homeodomains similar to *Emx2* (Stein and Kessel, 1995). Chicken *Cnot1* is expressed in prospective forebrain at the early neurula stage and later in the diencephalon. A *Not2* cognate, *floating head*, is essential for the development of the epiphysial region in zebrafish (Masai et al., 1997). However, no mouse *Not* homologues have been identified. The identification of a gene that complements *Emx2* using *Emx2* single mutants at the three- to four-somite stage is eagerly awaited, in addition to the examination of other possibilities.

REFERENCES

Acampora, D., Mazan, S., Lallemand, Y., Avantaggiato, V., Maury, M., Simeone, A. and Brulet, P. (1995). Forebrain and midbrain regions are deleted in $Otx2^{-/-}$ mutants due to a defective anterior neuroectoderm specification during gastrulation. *Development* **121**, 3279-3290.

Acampora, D., Mazan, S., Avantaggiato, V., Barone, P., Tuorto, F., Lallemand, Y., Brulet, P. and Simeone, A. (1996). Epilepsy and brain abnormalities in mice lacking the *Otx1* gene. *Nat. Genet.* **14**, 218-222.

Acampora, D., Avantaggiato, V., Tuorto, F. and Simeone, A. (1997). Genetic control of brain morphogenesis through *Otx* gene dosage requirement. *Development* **124**, 3639-3650.

Acampora, D., Avantaggiato, V., Tuotro, F., Briata, P., Corte, G. and Simeone, A. (1998). Visceral endoderm-restricted translation of *Otx1* mediates recovery of *Otx2* requirements for specification of anterior neural plate and normal gastrulation. *Development* **125**, 5091-5104.

Acampora, D., Avantaggiato, V., Tuorto, F., Barone, P., Perera, M., Choo, D., Wu, D., Corte, G. and Shimeone, A. (1999). Differential transcriptional control as the major molecular event in gene $Otx1^{-/-}$ and $Otx2^{-/-}$ divergent phenotypes. *Development* **126**, 1417-1426.

Ang, S.-L., Jin, O., Rhinn, M., Daorigle, N., Stevenson, L. and Rossant, J. (1996). A targeted mouse *Otx2* mutation leads to severe defects in gastrulation and formation of axial mesoderm and to deletion of rostral brain. *Development* **122**, 243-252.

Araki, I. and Nakamura, H. (1999). *Engrailed* defines the position of dorsal di-mesencephalic boundary by repressing diencephalic fate. *Development* **126**, 5127-5135.

Asano, M. and Gruss, P. (1992). *Pax-5* is expressed at the midbrain-hindbrain boundary during mouse development. *Mech. Dev.* **39**, 29-39.

Bally-Cuif, L., Cholley, B. and Wassef, M. (1995). Involvement of *Wnt-1* in the formation of the mes/metencephalic boundary. *Mech. Dev.* **53**, 23-34.

Bally-Cuif, L. and Wassef, M. (1995). Determination events in the nervous system of the vertebrate embryo. *Curr. Opin. Genet. Dev.* **5**, 450-458.

Barnes, J. D., Crosby, J. L., Jones, C. M., Wright, C. V. E. and Hogan, B. L. M. (1994). Embryonic expression of *Lim-1*, the mouse homolog of Xenopus *Xlim-1*, suggests a role in lateral mesoderm differentiation and neurogenesis. *Dev. Biol.* **161**, 168-178.

Beddington, R. S. P. and Robertson, E. J. (1998). Anterior patterning in mouse. *Trends Genet.* **14**, 277-284.

Beddington, R. S. P. and Robertson, E. J. (1999). Axis development and early asymmetry in mammals. *Cell* **96**, 195-209.

Boncinelli, S., Gulisano, M. and Broccoli, V. (1993). *Emx* and *Otx* homeobox genes in the developing mouse brain. *J. Neurobiol.* **24**, 1356-1366.

Broccoli, V., Boncinelli, E. and Wurst, W. (1999). The caudal limit of *Otx2* expression positions the isthmic organizer. *Nature* **401**, 164-168.

Bulfone, A., Puelles, L., Porteus, M. H., Frohman, M. A., Martin, G. R. and Rubenstein, J. L. R. (1993). Spatially restricted expression of *Dlx-1*, *Dlx-2 (Tes-1)*, *Gbx-2*, and *Wnt-3* in the embryonic day12.5 mouse forebrain defines potential transverse and longitudinal segmental boundaries. *J. Neurosci.* **13**, 3155-3172.

Cheng, H.-J. and Flanagan, J. G. (1994). Identification and cloning of *ELF-1*, a developmentally expressed ligand for *Mek4* and *Sek* receptor tyrosine kinases. *Cell* **79**, 157-168.

Cho, E. A. and Dressler, G. R. (1998). *TCF-4* binds beta-catenin and is expressed in distinct regions of the embryonic brain and limbs. *Mech. Dev.* **77**, 9-18.

Crossley, P. H. and Martin, G. R. (1995). The mouse *Fgf8* gene encodes a family of polypeptides and is expressed in regions that direct outgrowth and patterning in the developing embryo. *Development* **121**, 439-451.

Crossley, P. H., Martinez, Z. and Martin, G. R. (1996). Midbrain development induced by *FGF8* in the chick embryo. *Nature* **380**, 66-68.

Danielian, P. S. and McMahon, A. P. (1996). *Engrailed-1* as a target of the *Wnt-1* signaling pathway in vertebrate midbrain development. *Nature* **383**, 332-334.

Davis, C. A. and Joyner, A. L. (1988). Expression patterns of the homeo box-containing genes *En-1* and *En-2* and the proto-oncogene *int-1* diverge during mouse development. *Genes Dev.* **2**, 1736-1744.

Davis, C. A., Noble-Topham, S. E., Rossant, J. and Joyner, A. L. (1988). Expression of the homeo box-containing gene *En-2* delineates a specific region of the developing mouse brain. *Genes Dev.* **2**, 361-371.

Dressler, G. R., Deutsch, U., Chowdhury, K., Nornes, H. O. and Gruss, P. (1990). *Pax2*, a new paired-box-containing gene and its expression in the developing excretory system. *Development* **109**, 787-795.

Echelard, Y., Vassileva, G. and McMahon, A. P. (1994). Cis-acting regulatory sequences governing *Wnt-1* expression in the developing mouse CNS. *Development* **120**, 2213-2224.

Eisenstat, D. D., Liu, J. K., Mione, M., Zhong, W., Yu, G., Anderson, S. T., Ghattas, I., Puelles, L. and Rubenstwin, J. L. R. (1999). *DLX-1, DLX-2*, and *DLX-5* expression define distinct stages of basal forebrain differentiation. *J. Comp. Neurol.* **414**, 217-237.

Ericson, J., Muhr, J., Placzek, M., Lints, T., Jessell, T. M. and Edlund, T. (1995). *Sonic Hedgehog* induces the differentiation of ventral forebrain neurons: A common signal for ventral patterning within the neural tube. *Cell* **81**, 747-756.

Feldheim, D. A., Vanderhaeghen, P., Hansen, M. J., Frisen, J., Lu, Q., Barbacid, M. and Flanagan, J. G. (1998). Topographic guidance labels in a sensory projection to the forebrain. *Neuron* **21**, 1303-1313.

Feldheim, D. A., Kim, Y.-I., bergemann, A. D., Frisen, J., Barbacid, M. and Flanagan, J. G. (2000). Genetic analysis of *ephrin-A2* and *ephrin-A5* shows their requirement in multiple aspects of retinocollicular mapping. *Neuron* **25**, 563-574.

Figdor, M. and Stern, C. D. (1993). Segmental organization of embryonic diencephalon. *Nature* **363**, 630-634.

Flenniken, A. M., Gale, N. W., Yancopoulos, G. D. and Wilkinson, D. G. (1996). Distinct and overlapping expression patterns of ligands for Eph-related receptor tyrosine kinases during mouse embryogenesis. *Dev. Biol.* **179**, 382-401.

Fujii, T., Pichel, J. G., Taira, M., Toyama, R. and Dawid, I. B. (1994). Expression patterns of the murine LIM classs homeobox gene *lim1* in the developing brain and excretory system. *Dev. Biol.* **199**, 73-83.

Garel, S., Marin, F., Mattei, M.-G., Vesque, C., Vincent, A and Charnay, P. (1997). Family of *Ebf/Olf-1*-related genes potentially involved in neuronal differentiation and regional specification in the central nervous system. *Dev. Dyn.* **210**, 191-205.

Gurdon, J. B., Partington, G. A. and De Robertis, E. M. (1976). Injected nuclei in frog oocytes: RNA synthesis and protein exchange. *J. Embryol. Exp. Morphol.* **36**, 541-553.

Grindley, J. C., Hargett, L. K., Hill, R. E., Ross, A. and Horgan, B. L. M. (1997). Disruption of *Pax6* function in homozygous for the $Pax6^{Sey-1Neu}$ mutation produces abnormalities in the early development and regionalization of the diencephalon. *Mech. Dev.* **64**, 111-126.

Hallonet, M. E. R., Hollemann, T., Wehr, R., Jenkins, N. A., Copeland, N. G., Pieler, T. and Gruss, P. (1998). *Vax1* is a novel homeobox-containing gene expressed in the developing anterior ventral forebrain. *Development* **125**, 2599-2610.

Hanks, W., Wurst, W., Anson-Cartwright, L., Suerbach, A. B. and Joyner, A. L. (1995). Rescue of the *En-1* mutant phenotype by replacement of *En-1* with *En-2*. *Science* **269**, 679-682.

Hidalgo-Sanchez, M., Simeone, A. and Alvarado-Mallart, R. (1999). *Fgf8* and *Gbx2* induction concomitant with *Otx2* repression is correlated with midbrain-hindbrain fate of caudal prosencephalon. *Development* **126**, 3191-3203.

Iler, N., Rowitch, D. H., Echelad, Y., McMahon, A. P. and Abate-Shen, C. (1995). A single homeodomain binding site restricts spatial expression of *Wnt-1* in the developing brain. *Mech. Dev.* **53**, 87-96.

Inoue, T., Nakamura, S. and Osumi, N. (2000). Fate mapping of the mouse prosencephalic neural plate. *Dev. Biol.* **219**, 373-383.

Joyner, A. L., Herrup, K., Auerbach, A., Davis, C. A. and Rossant, J. (1991). Subtle cerebellar phenotype in mice homozygous for a targeted deletion of the *En-2* homeobox. *Science* **251**, 1239-1243.

Joyner, A. L. (1996). *Engrailed, Wnt* and *Pax* genes regulate midbrain-hindbrain development. *Trends Genet.* **12**, 15-20.

Kimura, C., Takeda, N., Suzuki, M., Oshimura, M., Aizawa, S. and Matsuo, I. (1997). Cis-acting elements conserved between mouse and pufferfish *Otx2* genes govern the expression in mesencephalic neural crest cells. *Development* **124**, 3929-3941.

Kimura, C., Yoshinaga, K., Tian, E., Suzuki, M., Aizawa, S. and Matsuo, I. (2000). Visceral endoderm mediates forebrain development by suppressing posteriorizing signals. *Dev. Biol.* **225**, 304-321.

Korinek, V., Barker, N., Willert, K., Molenar, M., Roose, J., Wagenaar, G., Markman, M., Lamers, W., Drestree, O. and Clevers, H. (1998). Two members of the *Tcf* family implicated in *Wnt/β-catenin* signaling during embryogenesis in the mouse. *Mol. Cell. Biol.* **18**, 1248-1256.

Lee, S. M., Danielian, P. S., Fritzsch, B. and McMahon, A. P. (1997). Evidence that *FGF8* signalling from the midbrain-hindbrain junction regulates growth and polarity in the developing midbrain. *Development* **124**, 959-969.

Liu, A. and Joyner, A. L. (2001). EN and GBX2 play essential roles downstream of FGF8 in patterning the mouse mid/hindbrain region. *Development* **128**, 181-191.

Mahmood, R., Bresnick, J., Hornbruch, A., Mahony, C., Morton, N., Colquhou, K., Martin, P., Lumsden, A., Dickson, C. and Mason, I. (1995). A role for *FGF-8* in the initiation and maintenance of vertebrate limb but outgrowth. *Curr. Biol.* **5**, 797-806.

Mallamaci, A., DiBlas, E., Brista, P., Boncinelli, E. and Corte, G. (1996). *Otx2* homeoprotein in developing central nervous system and migratory cells of the olfactory area. *Mech. Dev.* **58**, 165-178.

Mallamaci, A., Iannone, R., Briata, P., Pintonello, L., Mercurio, S., Boncinelli, E. and Corte, G. (1998). *Emx2* protein in the developing mouse brain and olfactory area. *Mech. Dev.* **77**, 165-172.

Martinez, S., Crossley, P. H., Cobos, I., Rubenstein, J. L. R. and Martin, G. R. (1999). *FGF8* induces formation of an ectopic isthmus organizer and isthmocerebellar development via a repressive effect on *Otx2* expression. *Development* **126**, 1189-1200.

Martinez, S. and Puelles, L. (2000). Neurogenetic compartments of the mouse diencephalon and some characteristic gene expression patterns. In *Mouse Brain Development*:; *Resuts and Problems in Cell Differentiation*. Vol. 30 (ed. M. Goffinet and P. Rakic), pp. 91-106. New York: Springer Life Sciences.

Martinez-Barbera, J. P., Rodriguez, T. A. and Beddington, R. S. (2000a). The homeobox gene *Hesx1* is required in the anterior neural ectoderm for normal forebrain formation. *Dev. Biol.* **223**, 422-430.

Martinez-Barbera, J. P., Clements, M., Thomas, P., Rodriguez, T., Meloy, D., Kioussis, D. and Beddington, R. S. (2000b). The homeobox gene *Hex* is required in definitive endodermal tissues for normal forebrain, liver and thyroid formation. *Development* **127**, 2433-2445.

Masai, I., Heisenberg, C. P., Barth, K. A., Macdonald, R., Adamek, S. and Wilson, S. W. (1997). Floating head and masterblind regulate neuronal patterning in the roof of the forebrain. *Neuron* **18**, 43-57.

Mastick, G. S., Davis, N. M., Andrews, G. L. and Easter, S. S., Jr (1997). *Pax-6* functions in boundary formation and axon guidance in the embryonic mouse forebrain. *Development* **124**, 1985-1997.

Matsunaga, E., Araki, I. and Nakamura, H. (2000). *Pax* defines the di-mesencephalic boundary by repressing *En1* and *Pax2*. *Development* **127**, 2357-2365.

Matsuo, I., Kuratani, S., Kimura, C., Takeda, N. and Aizawa, S. (1995). Mouse *Otx2* functions in the formation and patterning of rostral head. *Genes Dev.* **9**, 2646-2658.

McMahon, A. P. and Bradley, A. (1990). The *Wnt-1* (*int-1*) proto-oncogene is required for development of a large region of the mouse brain. *Cell* **62**, 1073-1085.

McMahon, A. P., Loyner, A. L., Bradley, A. and McMahon, J. A. (1992). The midbrain-hindbrain phenotype of *Wnt-1*⁻/⁻ mice results from stepwise deletion of *engrailed*-expressing cells by 9.5 days postcoitum. *Cell* **69**, 581-595.

Millen, K. J., Wurst, W., Herrup, K. and Joyner, A. (1994). Abnormal embryonic cerebellar development and patterning of postnatal foliation in two mouse *Engrailed-2* mutants. *Development* **120**, 695-706.

Millet, S., Campbell, K., Epstein, D. J., Losos, K., Harris, E. and Joyner, A. L. (1999). A role for *Gbx2* in repression of *Otx2* and positioning the mid/hindbrain organizer. *Nature* **401**, 161-164.

Miyamoto, N., Yoshida, M., Kuratani, S., Matsuo, I. and Aizawa, S. (1997). Defects of urogenital development in mice lacking *Emx2*. *Development* **124**, 1653-1664.

Nada, S., Yagi, T., Takeda, N., Tokunaga, H., Nakagawa, Y., Ikawa, Y., Okada, M. and Aizawa, S. (1993). Constitutive activation of *Src* family kinases in mouse embryos that lack *Csk*. *Cell* **73**, 1125-1135.

Nakano, T., Murata, T., Matsuo, I. and Aizawa, S. (2000). *O*TX2 directly interacts with lim1 and HNF-3β. *Biochem. Biophys. Res. Commun.* **267**, 64-70.

Ohsaki, K., Morimitsu, T., Ishida, Y., Kominami, R. and Takahashi, N. (1999). Expression of the *Vax* family homeobox genes suggests multiple roles in eye development. *Genes Cells* **4**, 267-276.

Oliver, G., Mailhos, A., Wehr, R., Copeland, G. N., Jenkins, A. N. and Gruss, P. (1995). *Six3*, a murine homologue of the sine oculis gene, demarcates the most anterior border of the developing neural plate and is expressed during eye development. *Development* **121**, 4045-4055.

Parr, B. P., Shea, M. J., Vassileva, G. and McMahon, A. P. (1993). Mouse *Wnt* genes exhibit discrete domains of expression in the early embryonic CNS and limb buds. *Development* **119**, 247-261.

Pellegrini, M., Mansouri, A., Simeone, A., Boncinelli, E. and Gruss, P. (1996). Dentate gyrus formation requires *Emx2*. *Development* **122**, 3893-3898.

Puelles, L. and Rubenstein, J. L. R. (1993). Expression pattern of homeobox and other putative regulatory genes in the embryonic mouse forebrain suggest a neuromeric organization. *Trends Neurosci.* **16**, 472-479.

Qiu, Y., Cooney, A. J., Kuratani, S., DeMayo, F. J., Tsai, S. Y. and Tsai, M.-J. (1994). Spatiotemporal expression patterns of chicken ovalbumin upstream promoter-transcription factors in the developing mouse central nervous system: evidence for a role in segmental patterning of the diencephalon. *Proc. Natl. Acad. Sci. USA* **91**, 4451-4455.

Qiu, M., Anderson, S., Chen, S., Meneses, J. J., Hevner, R., Kuwana, E., Pedersen, R. A. and Rubenstein, J. L. R. (1996). Mutation of the *Emx-1* homeobox gene disrupts the corpus callosum. *Dev. Biol.* **178**, 174-178.

Rhinn, M., Dierich, A., Shawlot, W., Behringer, R. R., Meur, M. L. and Ang, S.-L. (1998). Sequential roles for *Otx2* in visceral endoderm and neuroectoderm for forebrain and midbraimn induction and specification. *Development* **125**, 845-856.

Rowitch, D. H. and McMahon, A. P. (1995). *Pax-2* expression in the murine neural plate precedes and encompasses the expression domains of *Wnt-1* and *En-1*. *Mech. Dev.* **38**, 3-8.

Royet, J. and Finkelstein, R. (1995). Pattern formation in Drosophila head development: the role of the orthodenticle homeobox gene. *Development* **121**, 3561-3572.

Rubenstein, J. L. R., Martinez, S., Shimamura, K. and Puelles, L. (1994). The embryonic vertebrate forebrain: the Prosomeric model. *Science* **266**, 578-580.

Rubenstein, J. L. R. and Shimamura, K. (1998). Regionalization of the prosencencephalic neural plate. *Annu. Rev. Neurosci.* **21**, 445-477.

Rubenstein, J. L. R., Shimamura, K., Martinez, S. and Puelles, L. (1998). Regionalization of the prosencephalic neural plate. *Annu. Rev. Neurosci.* **21**, 445-477.

Sakai, K. and Miyazaki, J. (1997). A transgenic mouse line that retains *Cre* recombinase activity in mature oocytes irrespective of the *cre* transgene transmission. *Biochem. Biophys. Res. Commun.* **237**, 318-324.

Schwarz, M., Alvarez-Bolado, G., Dressler, G., Urbanek, P., Busslinger, M. and Gruss, P. (1999). *Pax2/5* and *Pax6* subdivide the early neural tube into three domains. *Mech. Dev.* **82**, 29-39.

Shamim, H., Mahmood, R., Logan, C., Doherty, P., Lumsden, A. and Mason, I. (1999). Sequential roles for *Fgf4*, *En1* and *Fgf8* in specification and regionalisation of the midbrain. *Development* **126**, 945-959.

Shawlot, W., Wakamia, M., Kwan, K. M., Kania, A., Jessell, T. M. and Behringer, R. R. (1999). *Lim1* is required in both primitive streak-derivatived tissues and visceral endoderm for head formation in the mouse. *Development* **126**, 4925-4932.

Shimamura, K., Hartigan, D., Martinez, S., Puelles, L. and Rubenstein, J. L. R. (1995). Longitudinal organization of the anterior neural plate and neural tube. *Development* **121**, 3923-3933.

Shimamura, K., Martinez, S., Puelles, L. and Rubenstein, J. L. R. (1997). Patterns of gene expression in the neural plate and neural tube subdivide the embryonic forebrain into transverse and longitudinal domains. *Dev. Neurosci.* **19**, 88-96.

Simeone, A., Gulisano, M., Acampora, D., Stornaiuolo, A., Rambaldi, M. and Boncinelli, E. (1992a). Two vertebrate homeobox genes related to the Drosophila *empty spiracles* gene are expressed in the embryonic cerebral cortex. *EMBO J.* **11**, 2541-2550.

Simeone, A., Acampora, D., Gulisano, M., Stornaiuolo, A. and Boncinelli, E. (1992b). Nested expression domains of four homeobox genes in developing rostral brain. *Nature* **358**, 687-690.

Simeone, A., Acampora, D., Mallamaci, A., Stornaiuolo, A., D'Apice, M. R., Nigro, V. and Boncinelli, E. (1993). A vertebrate gene related to *orthodenticle* contains a homeodomain of the bicoid class and demarcates anterior neuroectoderm of the gastrulating mouse embryo. *EMBO J.* **12**, 2735-2747.

Simeone, A. (2000). Positioning the isthmic organizer. Where *Otx2* and *Gbx2* meet. *Trend Genet*.**16**, 237-239.

Stein, S. and Kessel, M. (1995). A homeobox gene involved in node, notochord and neural plate formation of chick embryos. *Mech. Dev.* **49**, 37-48.

Stoykova, A., Fritssch, R., Walther, C. and Gruss, P. (1996). Forebrain patterning defects in small eye mutant mice. *Development* **122**, 3453-3465.

Stoykova, A., Gotz, M., Gruss, P. and Price, D. J. (1997). *Pax6*-dependent

regulation of adhesive patterning, *R-cadherin* expression and boundary formation in developing forebrain. *Development* **124**, 3765-3777.

Suda, Y., Matsuo, I., Kuratani, S. and Aizawa, S. (1996). *Otx1* function overlaps with *Otx2* in development of mouse forebrain and midbrain. *Genes Cells* **1**, 1031-1044.

Suda, Y., Matsuo, I. and Aizawa, S. (1997). Cooperation between *Otx1* and *Otx2* genes in developmental patterning of rostral brain. *Mech. Dev.* **69,** 125-141.

Suda, Y., Nakabayashi, J., Matsuo, I. and Aizawa, S. (1999). Functional equivalency between *Otx2* and *Otx1* in development of the rostral head. *Development* **124**, 743-757.

Tam, P. P. L. and Steiner, K. A. (1999). Anterior patterning by synergistic activity of the early gastrula organizer and the anterior germ layer tissues of the mouse embryo. *Development* **126**, 5171-5179.

Tanaka, S., Nomizu, M and Kurosumi, K. (1991). Intracellular sites of proteolytic processing of pro-opiomelanocortin in melanotrophs and corticotrophs in the rat pituitary. *J. Histochem. Cytochem.* **39,** 809-821.

Tao, W. and Lai, E. (1992). Telencephalon-restricted expression of *BF-1*, a new member of the *HNF-3/fork head* gene family, in the developing rat brain. *Neuron* **8**, 957-966.

Thomas, P. and Beddington, R. (1996). Anterior primitive endoderm may be responsible for patterning the anterior neural plate in the mouse embryo. *Curr. Biol.* **6**, 1487-1496.

Urbanek, P., Wang, Z., Fetla, I., Wagner, E. F. and Busslinger, M. (1994). Complete block of early B cell differentiation and altered patterning of the posterior midbrain in mice lacking *Pax5/BSAP*. *Cell* **79**, 901-912.

Urbanek, P., Fetka, I., Heisler, M. H. and Busslinger, M. (1997). Cooperation of *Pax2* and *Pax5* in midbrain and cerebellum development. *Proc. Natl. Acad. Sci. USA* **94**, 5703-5708.

Wallis, D. and Muenke, M. (2000). Mutation in holoprosencephaly. *Hum. Mutat.* **16**, 99-108.

Walther, C. and Gruss, P. (1991). *Pax-6*, a murine paired box gene, is expressed in_the developing CNS. *Development* **113**, 1435-1449.

Warren, N. and Price, D. J. (1997). Roles of *Pax-6* in murine diencephalic development. *Development* **124**, 1573-1582.

Wassarman. K. M., Lewandoski, M., Campbell, K., Joyner, A. L., Rubenstein, J. L., Martinez, S. and Martin, G. R. (1997). Specification of the anterior hindbrain and establishment of a normal mid/hindbrain organizer is dependent on Gbx2 gene function. *Development* **124**, 2923-2934.

Wilkinson, D. G. (1993). In situ hybridization. In *Essential Developmental Biology: A Practical Approach* (ed. C. D. Stern and P. W. H. Holland), pp. 257-274. Oxford: IRL Press.

Wurst, W., Auerbach, A. B. and Joyner, A. L. (1994). Multiple developmental defects in *Engrailed-1* mutant mice: an early mid-hindbrain deletion and patterning defects in forelimbs and sternum. *Development* **120**, 2065-2075.

Yagi, T., Tokunaga, T., Furuta, Y., Nada, S., Yoshida, M., Tsukada, T., Saga, Y., Takeda, N., Ikawa, Y. and Aizawa, S. (1993a). A novel ES cell line, TT2, with high germline-differentiating potency. *Anal. Biochem.* **214**, 70-76.

Yagi, T., Nada, S., Watanabe, N., Tamemoto, H., Kohmura, N., Ikawa, Y. and Aizawa, S. (1993b). A novel negative selection for homologous recombinants using diphtheria toxin A fragment gene. *Anal. Biochem.* **214**, 77-86.

Yoshida, M., Suda, Y., Matsuo, I., Miyamoto, N., Takeda, N., Kuratani, S. and Aizawa, S. (1997). *Emx1* and *Emx2* functions in development of dorsal mtelencephalon. *Development* **124**, 101-111.